Central CCL2 signaling onto MCH neurons mediates metabolic and behavioral adaptation to inflammation

Ophélia Le Thuc, Céline Cansell, Miled Bourourou, Raphaël Gp Denis, Katharina Stobbe, Nadège Devaux, Alice Guyon, Julie Cazareth, Catherine Heurteaux, William Rostène, et al.

Scientific Report

SOURCE DATA | TRANSPARENT PROCESS

EMBO reports

Central CCL2 signaling onto MCH neurons mediates metabolic and behavioral adaptation to inflammation

Ophélia Le Thuc[1,2], Céline Cansell[1,2], Miled Bourourou[1,2], Raphaël GP Denis[3], Katharina Stobbe[1,2], Nadège Devaux[1,2], Alice Guyon[1,2], Julie Cazareth[1,2], Catherine Heurteaux[1,2], William Rostène[4], Serge Luquet[3], Nicolas Blondeau[1,2,†], Jean-Louis Nahon[1,2,5,**,†] & Carole Rovère[1,2,*,†]

Abstract

Sickness behavior defines the endocrine, autonomic, behavioral, and metabolic responses associated with infection. While inflammatory responses were suggested to be instrumental in the loss of appetite and body weight, the molecular underpinning remains unknown. Here, we show that systemic or central lipopolysaccharide (LPS) injection results in specific hypothalamic changes characterized by a precocious increase in the chemokine ligand 2 (CCL2) followed by an increase in pro-inflammatory cytokines and a decrease in the orexigenic neuropeptide melanin-concentrating hormone (MCH). We therefore hypothesized that CCL2 could be the central relay for the loss in body weight induced by the inflammatory signal LPS. We find that central delivery of CCL2 promotes neuroinflammation and the decrease in MCH and body weight. MCH neurons express CCL2 receptor and respond to CCL2 by decreasing both electrical activity and MCH release. Pharmacological or genetic inhibition of CCL2 signaling opposes the response to LPS at both molecular and physiologic levels. We conclude that CCL2 signaling onto MCH neurons represents a core mechanism that relays peripheral inflammation to sickness behavior.

Keywords CCL2 chemokine; CCR2 signaling pathway; melanin-concentrating hormone; neuroinflammation; weight loss

Subject Categories Immunology; Metabolism; Neuroscience

DOI 10.15252/embr.201541499 | Received 4 October 2015 | Revised 25 August 2016 | Accepted 30 August 2016 | Published online 12 October 2016

EMBO Reports (2016) 17: 1738–1752

Introduction

Sickness behavior refers to the broad metabolic and behavioral changes that develop over the course of illness in response to inflammatory stimuli. Among these, pro-inflammatory cytokines, such as interleukin-1 (IL-1), interleukin-6 (IL-6), and tumor necrosis factor-α (TNF-α), as well as chemokines, can directly alters mood, food intake, and body weight through local action onto central hypothalamic network regulation energy balance and stress response [1–4].

In visceral injuries, local production of cytokines can rapidly signal to the brain via a direct action onto primary afferent nerves, including the vagus and the trigeminal nerves. Following bacterial infection, activation of resident macrophages of the choroid plexus and of the circumventricular organs, devoid of blood–brain barrier (BBB), induces synthesis of pro-inflammatory cytokines that directly enter the brain. Peripheral cytokines may also cross the BBB using saturable transport systems or transitory local openings. Cytokine activation of perivascular macrophages and brain endothelial cells generates prostaglandins E2 that act on the hypothalamo–pituitary–adrenal axis to regulate stress responses [5]. Finally, the central nervous system (CNS) may synthesize *de novo* cytokines following systemic or central inflammation [6]. However, the cellular and molecular basis by which peripheral inflammation is integrated centrally to adapt food intake and body weight remains largely unknown.

Lipopolysaccharide (LPS), when injected peripherally, triggers all the key features of sickness behavior, that is, peripheral and central inflammation, suppression of appetite, and weight loss [7]. While the molecular underpinnings remain unknown, it has been shown that central, rather than peripheral, inflammation is mediating LPS-induced appetite and weight loss [8], and interestingly, CNS inflammation can be triggered independently from systemic cytokines, by non-hematopoietic cells of the brain expressing the LPS receptor: the Toll-like receptor 4 (TLR4) [9]. Central neural substrate regulating feeding and energy expenditure is composed of several neuropeptidergic circuits primarily located in the hypothalamus and brainstem. Among these, the "first-order" neuronal populations that lie close to circumventricular organs integrate circulating signals of hunger and satiety and represent also a target for peripheral inflammatory signals. They include both orexigenic/anabolic

1 Université Côte d'Azur, Nice, France
2 CNRS, IPMC, Sophia Antipolis, France
3 Univ Paris Diderot, Sorbonne Paris Cité, Unité de Biologie Fonctionnelle et Adaptative, CNRS UMR 8251, Paris, France
4 Institut de la Vision, UMRS 968-Université Pierre et Marie Curie, Paris, France
5 Station de Primatologie, UPS846 CNRS, Rousset-sur-Arc, France
*Corresponding author. Tel: +33 93957741; E-mail: rovere@ipmc.cnrs.fr
**Corresponding author. Tel: +33 93957753; E-mail: nahonjl@ipmc.cnrs.fr
†These co-authors share last author position

producing neuropeptide Y (NPY)/agouti-related polypeptide (AgRP) and anorectic/catabolic neurons that produce pro-opiomelanocortin (POMC)/cocaine- and amphetamine-regulated transcript (CART) in the arcuate nucleus (ARC). Once ARC neurons have integrated peripheral signals, they, in turn, project to "second-order" neurons located in various brain regions, including hypothalamic areas such as the lateral hypothalamic area (LHA), the ventromedial hypothalamic area (VMH), and the paraventricular nucleus (PVN) [10,11]. The hypothalamus–brainstem structure is referred as to the homeostatic circuitry and operates adaptive metabolic and behavioral responses that regulate body weight. [12].

Thus, it was tempting to speculate that central inflammatory signaling may temporarily alter "first-order" and "second-order" neurons to promote LPS-provoked weight loss. While few interleukins receptors were found on hypothalamic neurons [13,14], they are particularly lacking in the LHA neurons, whereas chemokine receptors are widely expressed and functional onto hypothalamic neurons [15], particularly the orexigenic melanin-concentrating hormone (MCH) [16–20] and the hypocretins/orexins (ORX) neurons [21].

We thus hypothesized that chemokines could be crucial intermediates connecting peripheral inflammation to the neuronal substrate mediating metabolic changes and anorexia associated with sickness behavior.

Among chemokines, we identified the monocyte chemoattractant protein 1 MCP-1/C-C motif chemokine ligand 2 (CCL2) as a potential key player because CCL2 is expressed in glial cells and discrete neuronal populations [22], is consistently increased in the CNS following peripheral inflammation [23], and has been shown to be crucially involved in LPS-mediated brain inflammation [24]. Using genetic, electrophysiological, and pharmacological approaches, we demonstrate that CCL2/CCR2 signaling onto MCH neurons is the core mechanism by which peripheral inflammatory response is centrally relayed to operate the behavioral and metabolic changes associated with sickness behavior.

Results

Systemic injection of LPS induces neuroinflammation and activates gene expression of neuropeptides involved in feeding behavior/energy balance

In order to fully characterize the sequence of molecular events that occurs at the central level in response to peripheral inflammation, we first studied the dose–response relationship of peripheral LPS injection on sickness behavior response. Intraperitoneal (ip) injection of 5 μg of LPS per mouse recapitulated most of the characteristic response seen in sickness behavior and was therefore selected for subsequent molecular analyses (Fig EV1A). We next performed a time-course study using targeted transcription profiling by PCR analysis study of pro-inflammatory cytokine genes (IL-1β, IL-6, TNF-α) and selected neuropeptide-encoding genes involved in feeding behavior to precise the molecular events that occur at hypothalamic level after ip LPS injection. As expected [25], ip LPS injection induced a very early (1–3 after post-injection) overexpression of the pro-inflammatory cytokine mRNAs (IL-1β, IL-6, TNF-α), with specific profiles (Fig EV1B). Ip LPS challenge also induced, 1 h after injection, a transitory, yet massive (up to 20-fold), induction of all the energy-related neuropeptide mRNA-encoding genes expressed in the ARC (POMC, CART, NPY, AgRP) (Fig EV1D). Strikingly, ip LPS injection induced a delayed and sustained decrease in MCH and ORX mRNA expression 24 and 48 h after injection (Fig EV1E).

Central inflammation mediated by LPS activates the expression of pro-inflammatory cytokines and CCL2 chemokine family

A dose of 500 ng of LPS per mouse injected centrally was selected based on its ability to recapitulate the time course of weight loss observed after peripheral injection (Fig 1A). Hypothalamic mRNA coding for cytokines and chemokines were quantified in a time window that precedes the first wave of increased cytokine gene expression and before downregulation of MCH or ORX gene expression, that is, 6 h after intracerebroventricular (icv) LPS or saline injection. LPS induced a sixfold to eightfold increase in mRNA-encoding IL-1β, IL-17A, and several other pro-inflammatory cytokines, including TNF-α (Fig 1B). Strikingly, the most robust activation of expression was found for genes encoding the CCL chemokines that bind to the CCR2 and/or CCR5 receptors (CCL2, CCL3, CCL4, CCL5, and CCL7 (Fig 1C)). As CCL2 plays a major role in brain inflammation following peripheral injection of LPS and selectively interacts with CCR2 in rodent brains [24,26,27], we focused on the CCL2/CCR2 signaling as a potential key mechanism relaying centrally the action of peripheral inflammation.

Central CCR2 signaling is required to operate metabolic and behavioral changes induced by LPS

Brain injection of 500 ng of LPS in WT mice induced a long-lasting decrease in body weight compared to saline-injected WT mice (Fig 2A and Appendix Fig S2). Pharmacologic or genetic blockade of CCL2/CCR2 signaling was achieved through either central CCR2 antagonist injection or in the genetic context of CCR2 KO mice. CCR2 antagonist-injected mice and genetic impairment of CCR2 signaling prevented LPS-induced weight loss with a maximum effect at the early times (6–8 h) and a late partial recovery (Fig 2A–C). As shown in the Figs EV2A and B and 2A and B, icv administration of CCR2 antagonist INCB3344 or genetic invalidation of CCR2 expression in mice induced a decrease in the percentage of weight loss of similar magnitude upon peripheral injection of LPS (Fig EV2A and B and Appendix Fig S1) or following icv LPS injection (Fig 2A and B) in mice.

Integrated analysis of energy homeostasis using indirect calorimetry coupled with activity and feeding measurement was used to fully characterize the physiologic implication of CCL2/CCR2 signaling in LPS-induced metabolic changes. Body weight loss following central LPS delivery was associated with a sharp decrease in food intake, energy expenditure, locomotor activity, and a metabolic shift toward lipid oxidation profile as indicated by both fat oxidation and respiratory quotient analysis (Figs 2 and EV3). Pharmacologically opposing CCR2 signaling through central delivery of the selective CCR2 antagonist INCB3344 [28] affected various aspects of LPS-induced weight loss. First, CCR2 antagonist counteracted the anorectic response initiated by LPS (Fig 2D and E) and mitigated the acute decrease in energy expenditure (Fig EV3C and D). Peripheral substrate utilization was calculated based on respiratory exchange ratio (VCO_2/VO_2: RER = 1 indicative of carbohydrate oxidation and RER = 0.7 indicative of lipid oxidation). Icv LPS injection induced a sharp shift in lipid oxidation

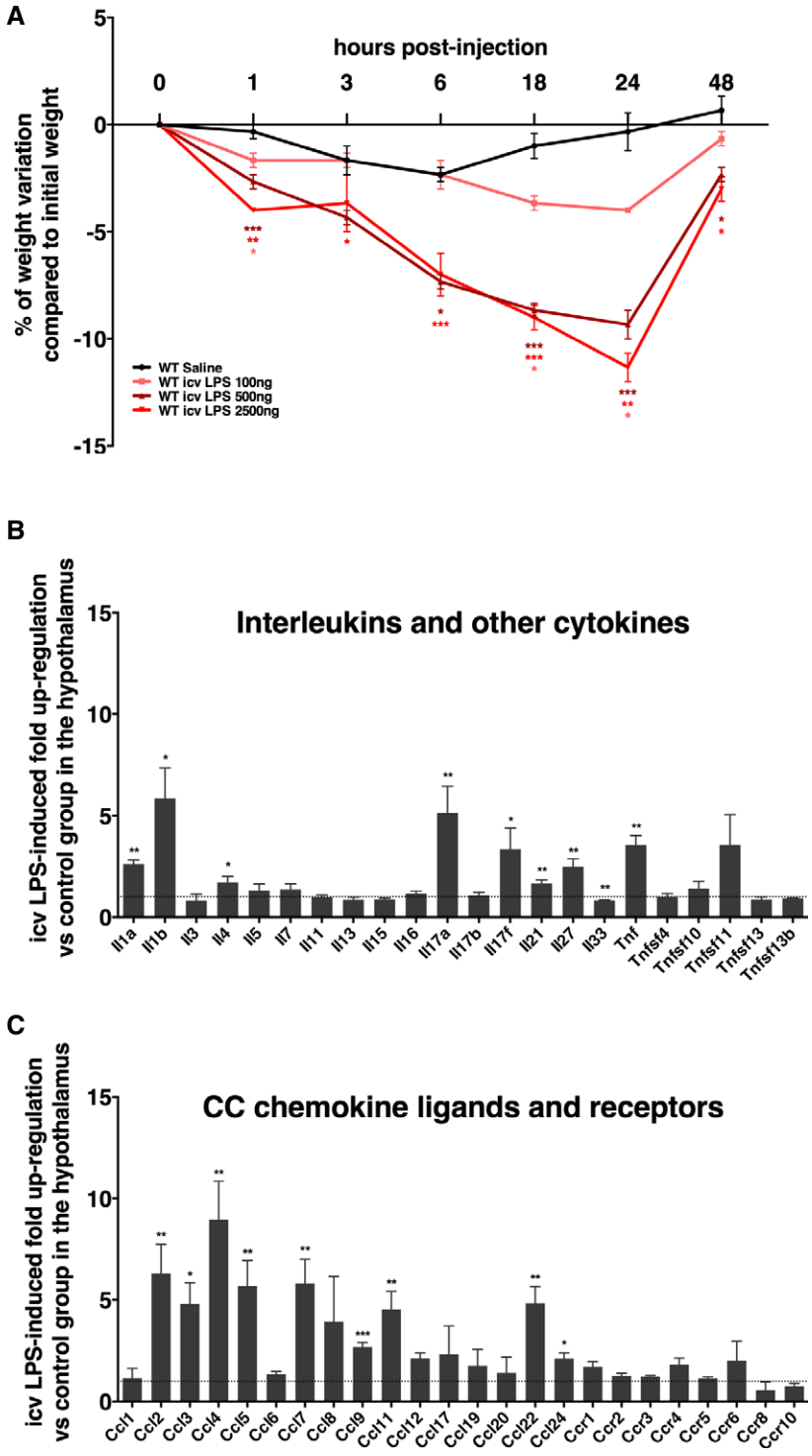

Figure 1. Analysis of inflammatory marker expression in icv LPS-injected mice.
See also Fig EV1.

A Dose–response relationship between icv LPS injection and mice weight loss (n = 3). Data are expressed as means ± SEM. *P < 0.05, **P < 0.01, ***P < 0.001; color-coded asterisks indicate a significant difference between the control saline condition and the experimental condition assigned to the respective color-coded curve.

B, C Analysis by real-time PCR. Arrays of interleukins, cytokines (B), and CC chemokine ligands and receptors (C) gene expression in the hypothalamus 6 h after an acute icv injection of LPS vs. saline in WT mice (n = 4–6 per group). LPS-induced fold upregulation vs. saline condition was calculated using the $\Delta\Delta C_T$ method according to the manufacturer's protocol. Data are expressed as means ± SEM. *P < 0.05; **P < 0.01, and ***P < 0.001.

Data information: Data were analyzed by Student's unpaired two-tailed t-test (A–C).
Source data are available online for this figure.

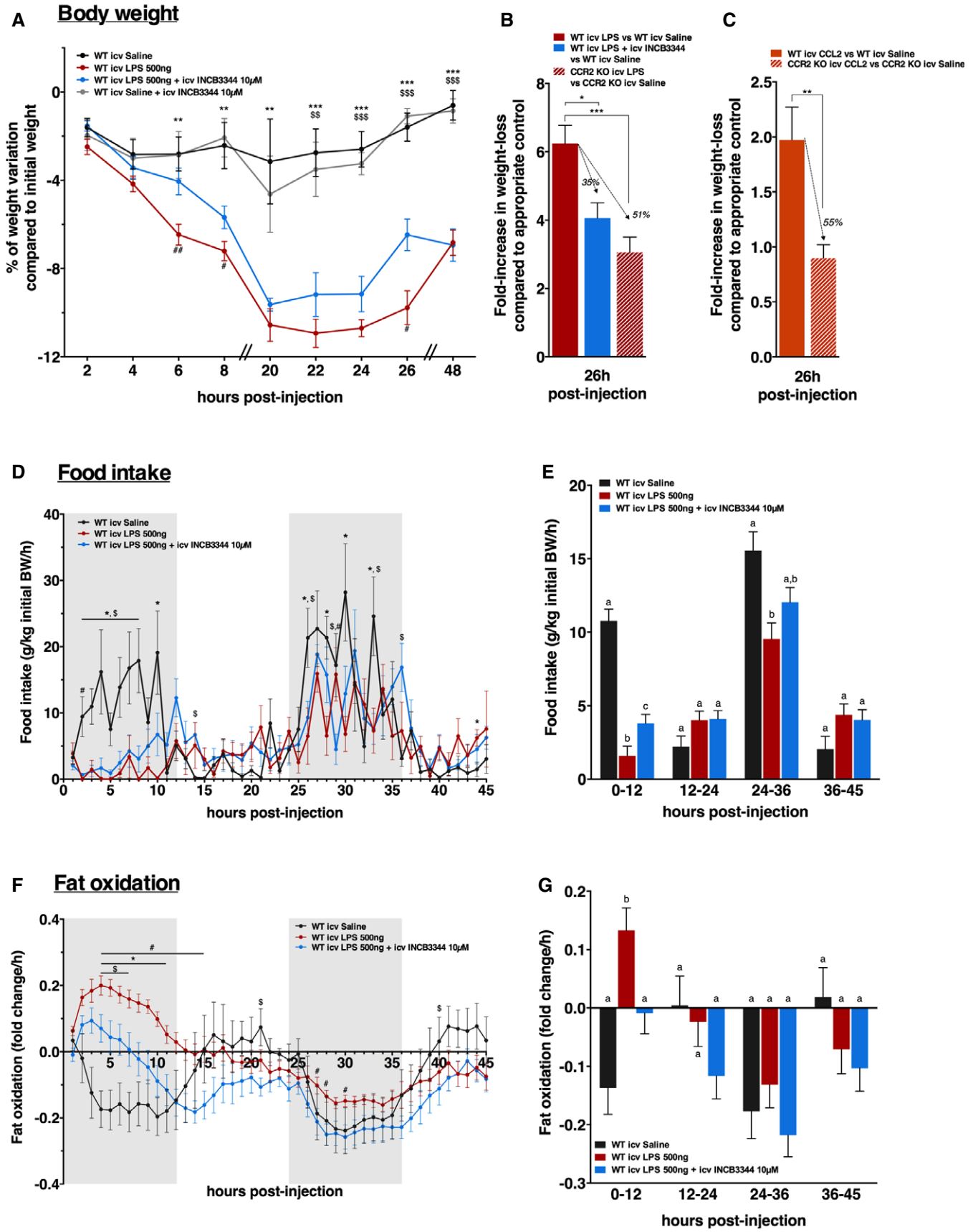

Figure 2.

Figure 2. LPS decreases body weight and food intake and increases fat oxidation activity through a CCR2-dependent mechanism.
See also Figs EV2 and EV3, Appendix Fig S2 and Appendix Table S2.

A Weight variation (%) compared to initial body weight at different times (from 2 to 48 h) after acute icv injection of saline (black curve), INCB3344 (gray curve), LPS (red curve) or LPS+INCB3344 (blue curve) in WT mice (n = 6–12).

B Fold increase in weight loss compared to appropriate saline-injected control 26 h after acute icv injection of LPS (red bar) or LPS+INCB3344 (blue bar) in WT mice or LPS in CCR2 KO mice (striped bar) (n = 6).

C Fold increase in weight loss compared to appropriate saline-injected control 26 h after acute icv injection of CCL2 in WT mice (orange bar) or in CCR2 KO mice (striped bar) (n = 6).

D Variation of food intake recorded for 45 h during light and dark period (gray area) after acute icv injection of saline (black curve), LPS (red curve), or LPS+INCB3344 (blue curve) in WT mice (n = 5–8).

E Food intake average over four periods of 12 h after acute icv injection of saline (black bars), LPS (red bars), or LPS+INCB3344 (blue bars) in WT mice (n = 5–8).

F Variation of fat oxidation recorded for 45 h during light and dark period (gray area) after acute icv injection of saline (black curve), LPS (red curve), or LPS+INCB3344 (blue curve) in WT mice (n = 5–8).

G Fat oxidation average over four periods of 12 h after acute icv injection of saline (black bars), LPS (red bars), or LPS+INCB3344 (blue bars) in WT mice (n = 5–8).

Data information: Data are expressed as means ± SEM. In (A–D and F), data were analyzed by Student's unpaired two-tailed t-test. $^{*,\$,\#}P < 0.05$; $^{**,\$\$,\#\#}P < 0.01$ and $^{***,\$\$\$,\#\#\#}P < 0.001$. * compares saline and LPS conditions; $^{\$}$ compares saline and LPS+INCB3344 conditions; and $^{\#}$ compares LPS and LPS+INCB3344 conditions. In (E and G), analyses of variances were performed followed by a Tukey's *post hoc* test with the appropriate parameters and their interaction as factor. Data with different superscript letters (a, b, c) differ significantly ($P < 0.05$).
Source data are available online for this figure.

profile (Figs 2F and G, and EV3E and F) and CCR2 signaling blockade protected fat stores while opposing this shift (Figs 2F and G, and EV3E and F). Importantly, the action of both LPS and CCR2 signaling could only be partially correlated to change in food intake and locomotor activity (Figs 2D and E, and EV3A and B). Those results indicate that central inflammation not only affects feeding but also peripheral nutrient partitioning in a CCR2-dependent manner.

Brain-injected LPS reduces MCH mRNA and peptide expression through CCR2 signaling

To study the molecular mechanisms involved in inflammation-induced weight loss and associated changes in energy balance at the brain level, and particularly at the hypothalamic level, we determined levels of mRNA-encoding cytokines (IL-1β, IL-6, TNF-α), 1, 3, 6, 18, and 24 h after icv injection of LPS, to cover primary responses, and 18 and 24 h after injection, to analyze secondary and counteractive responses. As shown in Fig 3A, IL-1β mRNA expression levels displayed two distinct waves that peaked at 3 and 18 h (23-fold) post-injection while IL-6 mRNA (16-fold) and TNF-α mRNA (sevenfold) levels were transitorily elevated at 3 h in the LPS-treated group as compared to the saline controls. We also determined the temporal patterns of CCL2 expression induced by icv injection of LPS and confirmed the strong upregulation of both gene and protein, 3 and 6 h after icv LPS (Fig 3B and C) and ip (Fig EV1C) injection, respectively.

For the neuropeptide-encoding mRNAs, there are differentiable responses following LPS icv injection. Robust (up to 12-fold) and transitory peak of induction was found for POMC (but not CART; Fig EV4A and B), whereas NPY (and also AgRP) mRNA expression was downregulated (twofold) at 1 h post-injection (Fig EV4C and D). In contrast, a late and sustained downregulation occurred for MCH mRNA (Fig 3D) and ORX (Fig EV5A) 18 and 24 h after LPS injection. We therefore characterized the protein levels of MCH and ORX and found that they followed the mRNA patterns observed at 1, 6, 18 h LPS post-injection. MCH (53.5 ± 5.2 ng/mg of proteins) (Fig 3E) and ORX (83.1 ± 2.1 ng/mg of proteins; Fig EV5B) dropped down compared to saline group at 18 h post-LPS. No change was observed for both neuropeptides in the cerebellum extracts used as negative controls (Figs 3E and EV5B).

Finally, we examined the relative importance of the CCR2 signaling pathway in the MCH-expressing neuronal network. Strikingly, the twofold decrease in MCH mRNA expression at 18 h LPS post-injection was reversed in mice treated with the selective CCR2 antagonist INCB3344 [28] and in CCR2 KO mice (at 81 and 77% of the initial MCH mRNA content, respectively) (Fig 3F). Strikingly, the 50% reduction in MCH mRNA expression was also similarly prevented under ip LPS administration (Fig EV2C). Altogether, these results suggest that CCR2 signaling could play a fundamental role in the LPS-based neuroinflammatory response leading to MCH gene downregulation.

Brain-injected CCL2 suppresses MCH mRNA and peptide expression through CCR2 signaling

We tested thereafter the hypothesis that a specific activation of CCR2 signaling may mimic the spectrum of cytokine/chemokine and neuropeptide gene expression variations observed following LPS treatment. We found that icv CCL2 injection increased mRNA coding for IL-1β, IL-6, and TNF-α by a 5.5-, 2.3- and 2.8-fold, respectively, at 6 h post-injection (Fig 4A). A fast (1 h) and long-lasting (up to 18 h) activation of both CCL2 mRNA and protein levels was also found in the hypothalamus (Fig 4B and C). Finally, expression of MCH or ORX-encoding mRNA was downregulated by 2.1- and 2.6-fold at 6 and 18 h, respectively (Figs 4D and EV5C). At the protein levels, CCL2 injection significantly decreased by twofold both MCH and ORX peptide concentrations compared to control group at 6 and 18 h post-injection (Figs 4E and EV5D). No change was observed for both neuropeptides in the cerebellum extracts used as negative controls (Figs 4E and EV5D).

Finally, the twofold decrease in MCH mRNA expression at 18 h LPS post-injection was blunted in CCR2 KO mice and in mice treated with INCB3344 (Fig 4F). This demonstrated that CCL2-induced MCH downregulation in the LHA was fully dependent upon the CCR2 signaling pathway.

CCR2 is expressed by MCH but not ORX neurons in the LHA of normal mice

As the distribution of CCR2 in normal rodent brain was poorly described [23], we characterized CCR2-immunoreactivity (CCR2-IR)

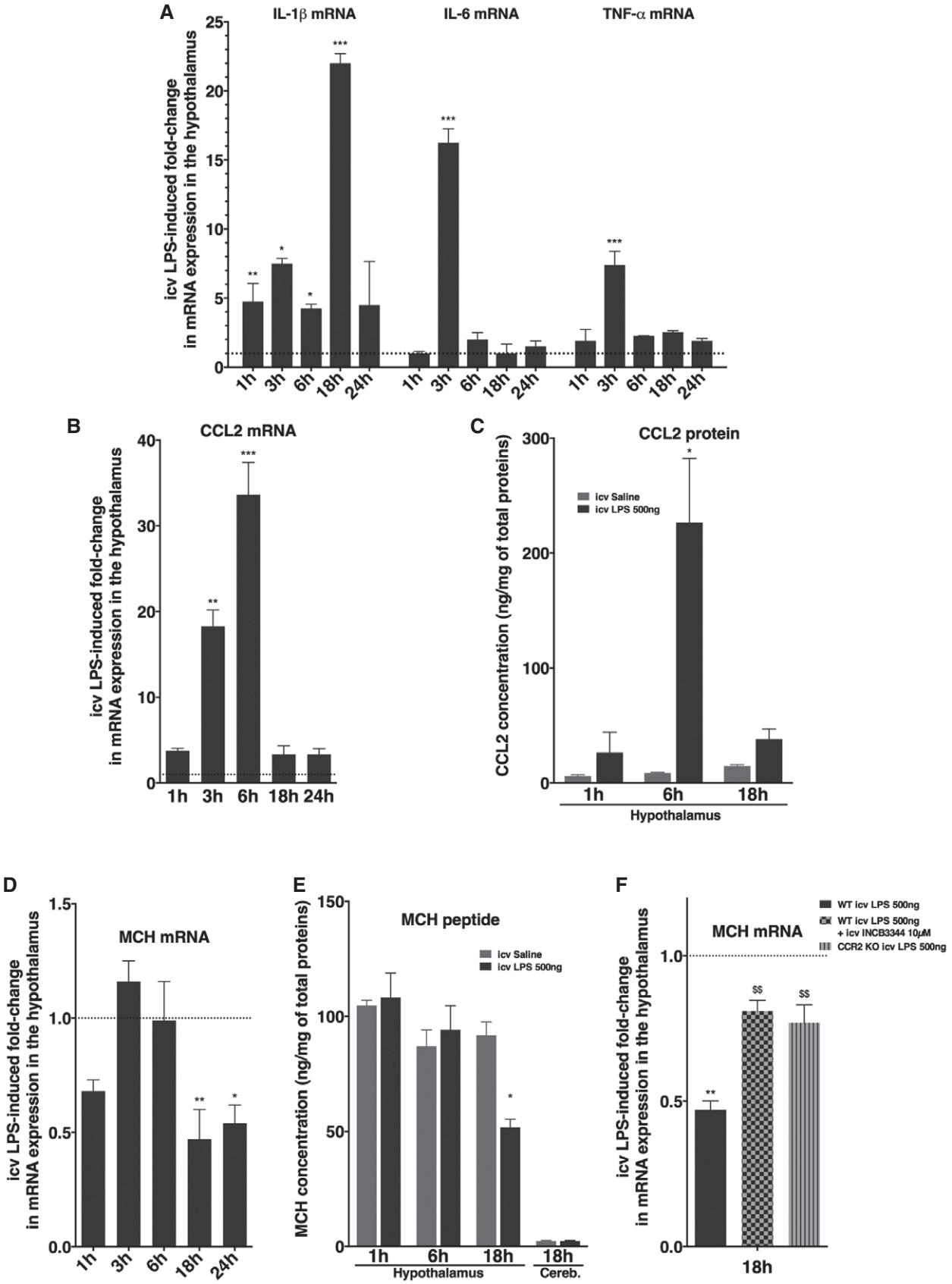

Figure 3.

Figure 3. Brain-injected LPS induced differential variations in hypothalamic expression of cytokines and of the orexigenic neuropeptide MCH.
See also Figs EV4 and EV5.

A Real-time PCR analysis of the genes coding for the pro-inflammatory cytokines IL-1β, IL-6, TNF-α in the hypothalamus of icv LPS-injected mice at different times after injection (from 1 h to 18 h), normalized to values in icv saline-injected mice (n = 6 per group).

B–E Study of gene and protein hypothalamic expression of the chemokine CCL2 (B, C) and MCH peptide (D, E) in icv LPS-injected mice. Real-time PCR analysis for CCL2 (B) and MCH (D) at different times after injection (from 1 to 24 h), normalized to values in control icv saline-injected mice (n = 6 per group). Measurement of CCL2 (C) and MCH (E) concentrations by EIA after icv LPS injection (black bars) or icv saline injection (gray bars) in mice at 1 h, 6 h and 18 h after injection. Cerebellum was used as negative control (3 independent experiments, n = 6 per group in each experiment).

F The decrease in MCH mRNA levels observed 18 h after icv LPS injection is partly abolished by the CCR2 antagonist INCB3344 (10 μM) and in CCR2 KO mice, as shown by real-time PCR analysis for MCH in the hypothalamus. Results were normalized to values in icv saline-injected WT mice (n = 6 per group). Data are expressed as means ± SEM. $^{**,\$\$}P < 0.01$. * saline vs. icv LPS injection in WT mice. $^{\$}$ icv LPS injection in WT mice vs. LPS+INCB3344 icv injection in WT mice or icv LPS injection in CCR2 KO mice.

Data information: Data in (A–E) are expressed as means ± SEM. $^{*}P < 0.05$, $^{**}P < 0.01$, $^{***}P < 0.001$, icv LPS injection vs. icv saline injection. Data were analyzed by Student's unpaired two-tailed t-test (A–F).

in mice expressing cyan fluorescent protein (CFP) under the control of the MCH promoter (MCH-CFP) [29,30]. MCH (green) and CCR2 (red) immunoreactivities largely overlapped demonstrating that most of the MCH neurons expressed CCR2 receptors (approximately 70%; Fig 5A), whereas CCR2-immunoreactivity was not found within ORX-expressing cells (Fig EV5E).

CCL2 directly hyperpolarizes MCH neurons in mouse brain slices

We performed patch-clamp experiments on fluorescent neurons expressing MCH of the lateral hypothalamic slices prepared from MCH-CFP mice. CCL2 application hyperpolarized MCH neurons (Fig 5B). CCR2 antagonist INCB3344 prevented CCL2-induced hyperpolarization (Fig 5B), and the hyperpolarization amplitude was dependent on CCL2 concentration (Fig 5C). It was of (absolute value in mV) 2.17 ± 0.94 at 0.1 nM CCL2, 3.45 ± 0.56 at 1 nM CCL2 and 5.63 ± 1.08 at 10 nM CCL2.

We investigated whether the hyperpolarization induced by CCR2 activation could be due to G protein activated inward rectifier current (GIRK) activation. The effect inverted around −80 mV that is the equilibrium potential for K^+ ions. We found that 1 nM CCL2 effect was significantly blocked by previous application of 200 μM barium, a concentration known to inhibit specifically KIR channels (Fig 5C). About 200 μM barium alone induced a significant depolarization of MCH neurons (of 10.00 ± 1.67 mV), suggesting that KIR channels are spontaneously opened under control conditions in MCH neurons. We then measured the current induced by CCL2 in voltage-clamp at a holding potential of −60 mV, with a KCl intracellular solution. CCL2 (10 nM) induced a small outward current (+7.5 ± 1.44 pA) associated with a decrease in membrane resistance (Fig EV6A and B). CCL2 (10 nM) also increased by 30% the frequency of spontaneous post-synaptic currents without significant effect on the amplitude of these events (Fig EV6C and D).

Finally, we investigated the consequences of the CCL2 effects on action potential (AP) discharge (Fig 5D). CCL2 induces either delays (Fig 5D, left panel) or failures (Fig 5D, right panel) in action potential emission. This effect was likely a consequence of a decrease in membrane resistance due to GIRK channels and/or receptor channels opening.

CCL2 abolishes KCl-induced MCH release from hypothalamic explants

Based on our observations of decrease in MCH neurons excitability, we evaluated whether CCL2 could modulate MCH release induced by a robust KCl-mediated neuronal depolarization. Perifusion of hypothalamic tissues with 60 mM KCl for 30 min induced a 3.1-fold increase in MCH release (Fig 5E, black line). Strikingly, this increase was fully blunted by co-application of CCL2 (Fig 5E, red line), an inhibitory effect reversed by addition of the CCR2 antagonist INCB3344 (Fig 5E, blue line). In contrast to MCH secretion, application of CCL2 did not prevent ORX release (Fig EV5F).

LPS or CCL2-induced weight loss may be driven by the MCH/MCHR1 signaling

Finally, we tested whether *in vivo* MCH signaling through MCHR1 was an important element to mediate LPS- or CCL2-induced weight loss (Fig 5F). In agreement with previous studies [18,31], the pharmacological inhibition of the MCH receptor by the specific antagonist H6408 blocked the basal orexigenic tone leading to a slight weight loss. LPS but not CCL2 injection doubled this response, suggesting a similar range of action for CCL2 or MCH antagonist on the weight loss. Similar effects were noted in presence or not of H6408 at both 6 and 24 h LPS post-injection. In contrast, an additive effect of the MCH antagonist was noted on the CCL2-driven weight loss at 6 h but not 24 h, highly suggesting that the MCH signaling pathway could participate as a major downstream element at this early time.

Discussion

While a participation of the ARC was established in inflammation-induced anorexia or weight loss [32–34], a contribution of LHA neurons expressing orexigenic neuropeptides like MCH or orexins could also be considered [35,36]. Furthermore, brain CCL2/CCR2 signaling is activated by systemic LPS injection [24,26].

Here, we demonstrated that LPS-induced behavioral and metabolic adaptation resulting in weight loss depends on the integrity of the CCR2 signaling in MCH-expressing neurons and revealed for the first time that locally produced brain chemokines may act directly on appetite-regulating neuronal networks. Brain inflammation was induced by ip and icv injections of LPS, as confirmed by an upregulation of cytokines such as IL-1β, that followed the characteristic two wave patterns observed after peripheral LPS injection [37]. Beneficial and detrimental effects of IL-1β production have been linked to neuroinflammatory conditions and neurodegenerative diseases. The molecular steps leading to IL-1β maturation take place

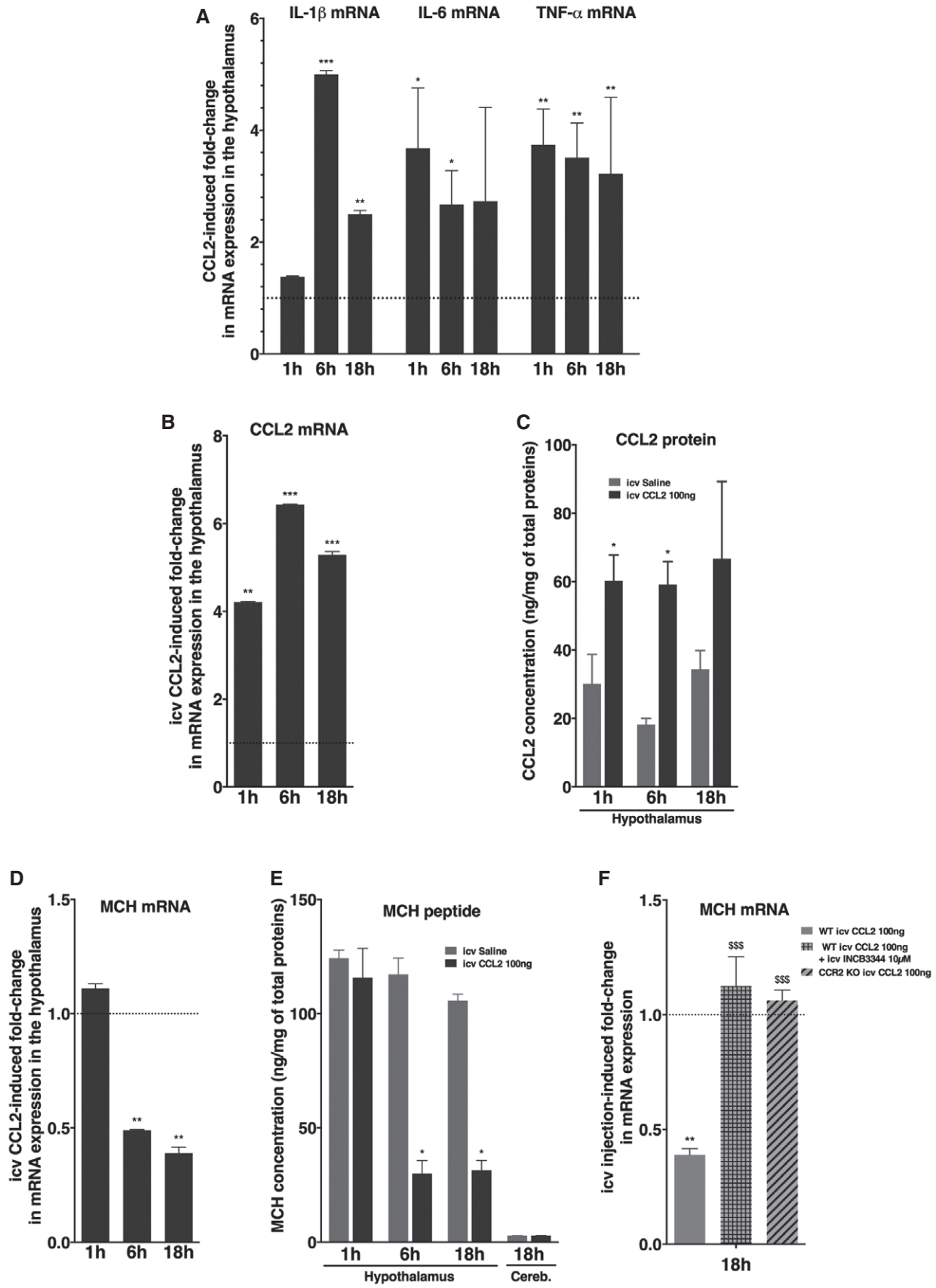

Figure 4.

Figure 4. Brain-injected CCL2 altered the expression of pro-inflammatory cytokines and of the orexigenic neuropeptide MCH in the hypothalamus.
See also Fig EV5.

A Real-time PCR analysis of the genes coding for the pro-inflammatory cytokines IL-1β, IL-6, TNF-α in the hypothalamus of icv CCL2-injected mice at different times after injection (from 1 to 18 h), normalized to values in icv saline-injected mice (n = 6 per group).

B–E Study of gene and protein hypothalamic expression of the chemokine CCL2 (B, C) and MCH peptide (D, E) in icv CCL2-injected mice. Real-time PCR analysis for CCL2 (B) and MCH (D) at different times after injection (from 1 h to 24 h), normalized to values in control icv saline-injected mice (n = 6 per group). Measurement of CCL2 (C) and MCH (E) concentration by EIA after icv CCL2 injection (black bars) or icv saline injection (gray bars) in mice at 1, 6, and 18 h after injection. Cerebellum was used as negative control (3 independent experiments, n = 6 per group in each experiment).

F The decrease in MCH mRNA levels observed 18 h after icv CCL2 injection is abolished by the CCR2 antagonist INCB3344 (10 μM) and in CCR2 KO mice, as shown by real-time PCR analysis for MCH in the hypothalamus. Results were normalized to values in icv saline-injected WT mice (n = 6 per group). $^{**}P < 0.01$, $^{\$\$\$}P < 0.001$. * saline vs. icv CCL2 injection in WT mice. $^{\$}$ icv CCL2 injection in WT mice vs. CCL2+INCB3344 icv injection in WT mice or icv CCL2 injection in CCR2 KO mice.

Data information: Data are expressed as means ± SEM. Data in (A–E): $^{*}P < 0.05$, $^{**}P < 0.01$, $^{***}P < 0.001$; icv CCL2 injection vs. icv saline injection. Data were analyzed by Student's unpaired two-tailed t-test (A–F).

in an intracellular complex termed the inflammasome [38]. However, the potential role of the NLRP3 inflammasome in the local production of IL-1β in the brain is not well understood [39,40]. In spite of our results linking acute inflammation and weight loss, it is tempting to speculate a role of NLRP3 inflammasome that would be interested to further investigate.

The central inflammation was associated with a striking increase in many CCR2 ligands. Among potential candidates, CCL2 was particularly considered, based on (i) its strong brain expression following systemic LPS challenges [25,26,41], (ii) its key role in the recruitment of monocytes in the brain [42,43], and (iii) the fact that both brain inflammation and weight loss following peripheral LPS injection are markedly reduced in CCL2 KO [24], CCR2 KO, and INCB3344-treated mice (Fig EV2 and Appendix Fig S2). Furthermore, CCL2 and CCR2 are expressed in LHA neurons [22,44], in contrast to sporadic cytokine receptors expression [13,14]. Therefore, we investigated whether CCL2 would act as intermediate between cytokines and neurons in the cascade linking inflammation to alteration of neuronal networks involved in food behavior. Firstly, its particular kinetics of activation following central LPS injection arises between inflammatory cytokines activation and downregulation of orexigenic peptides, such as MCH and ORX. Secondly, its primary receptor, CCR2 is expressed into MCH-producing neurons leading to hypothesize that CCL2 could directly modulate MCH neurons activity. Indeed, in mice with genetic or pharmacological CCR2 disruption, ip and icv LPS injections were inefficient in reducing MCH mRNA. Such mandatory effect of CCL2/CCR2 signaling on MCH gene regulation was confirmed by the full reversion of CCL2-induced MCH mRNA decrease in the CCR2 KO and INCB3344-treated mice. The 50% reduction in MCH mRNA expression was similarly prevented in both paradigms either under ip or under icv LPS administration (Figs EV2C and 3F). The same responses noted under both types of injection indicate that weight loss following icv LPS administration could not result from a general noxious action.

CCL2 generates a hyperpolarization blocked by low barium concentration associated with an increase in membrane conductance, characteristic of activation of a GIRK current. This will tend to shunt somatic excitatory currents and block the propagation of excitatory events. Indeed, CCL2, via the direct stimulation of CCR2, depresses the frequency of discharge of evoked APs. Finally, we addressed the effect of CCL2 on the release of MCH induced by KCl-mediated depolarization [45]. We found a drastic reduction in MCH secretion by adding CCL2, an effect fully blocked by the INCB3344 antagonist.

Intriguingly, further MCH secretion induced by KCl-mediated depolarization was observed in the only presence of the INCB3344 antagonist (data not shown) suggesting that endogenous CCL2 may also contribute to the strong inhibition of MCH release. As a significant proportion of MCH neurons expresses both CCR2 and CCL2 and could be activated by the general depolarization induced by KCl, the locally expressed chemokine would act as a short-loop autocrine modulator amplifying the CCL2 responses driven by astrocyte activation [42,46]. Thus, both sources of brain CCL2 are likely to contribute to the inhibition of MCH secretion.

Among the myriad of mediators involved in the LPS-driven brain inflammation that modifies the activity of neurons [47–50], we demonstrated here that CCL2/CCR2 signaling could directly inhibit a major orexigenic neuronal network, that is, the MCH neuronal pathway.

As CCL2 effects on feeding behavior and body weight were poorly investigated [51], this study is the first demonstrating selective weight loss following icv CCL2 injection in mice, an effect fully abolished in CCR2 KO mice or mice treated with the CCR2 antagonist. Interestingly, extensive analysis of the different metabolic parameters affected by central inflammation also revealed that not only food intake but also peripheral nutrient partitioning is affected by LPS injection and rely onto CCL2 signaling.

Prevention of the weight loss induced by LPS by CCR2 antagonist injection or invalidation of the CCR2 gene in transgenic mice was partial and transitory, indicating that there must be other neuronal pathways involved in this action. Indeed, LepR/γ-aminobutyric acid (GABA)-expressing neurons have been shown to also regulate body weight: leptin mainly acts on GABAergic neurons to reduce body weight and triggers POMC neuronal activity by reducing GABA release onto these neurons. This suggested a body weight-promoting role for GABA released from leptin-inhibited neurons [52–54]. Since ORX neurons do not express CCR2, the few $MCH^{-}/CCR2^{+}$ cells we noticed in the LHA could be related to LepR/GABA neuronal pathway. Importantly, MCH neurons are located in the LHA which is known to be a pre-ganglionic structure whose output directly affects neurons controlling autonomic output, which in turn controls peripheral substrate utilization [55]. Hence, MCH neurons could relay two of the main adaptive responses triggered by central inflammation, that is, reduction in appetite and loss of fat stores through enhanced fat oxidation. Paradoxically, CCR2 signaling is involved in metabolic disorders associated with obesity [56] as underlined by its role in the hyperphagic response to a high-fat diet (HFD) [57], as another chemokine system, the CXCL12/CXCR4 system. Thus, these chemokine systems may have a role in mediating both neuronal and behavioral effects induced by a HFD [58]. Nevertheless, a low-grade inflammation both in the CNS and at the

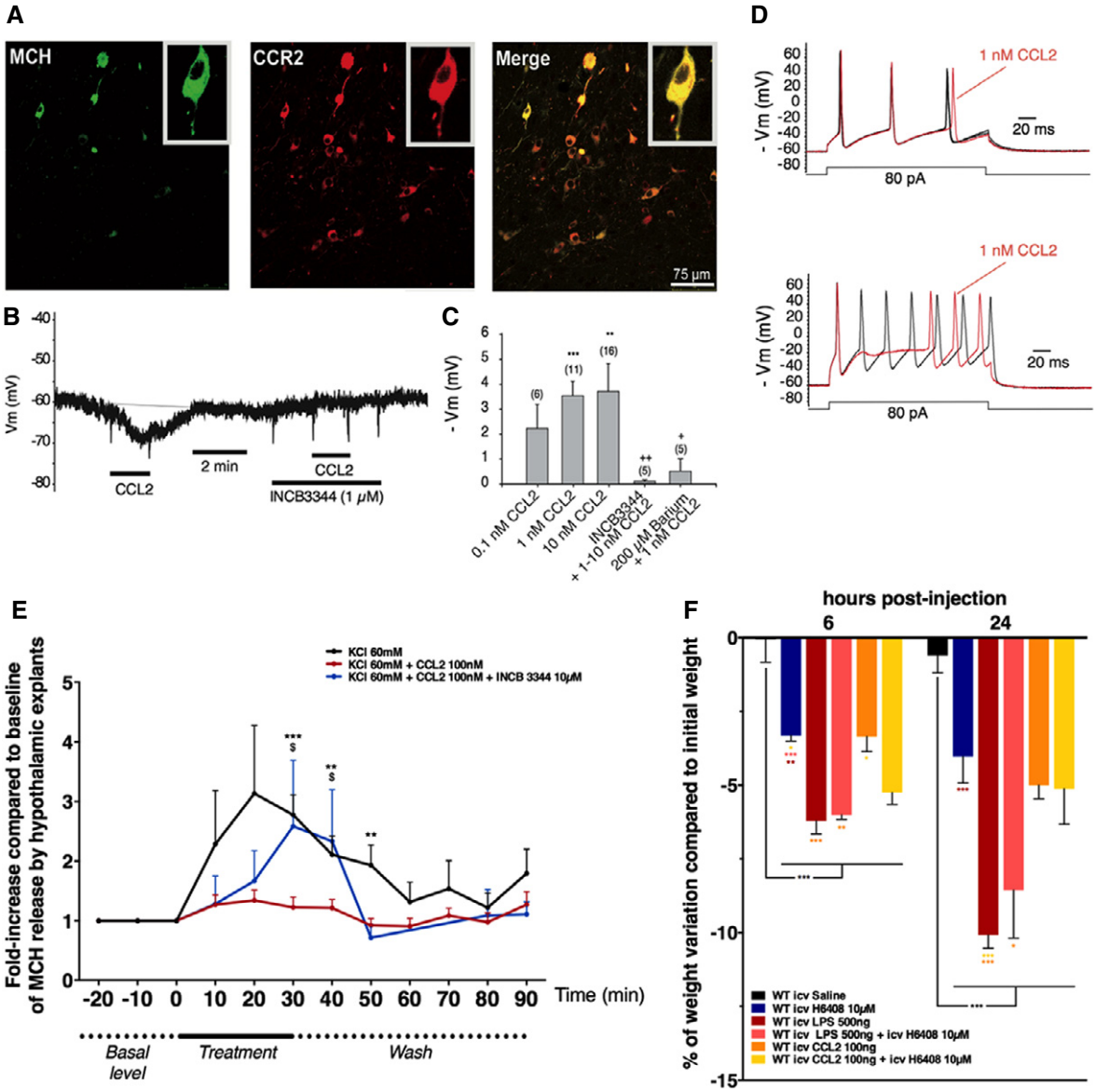

Figure 5. The chemokine CCL2 can directly modulate MCH neurons.

See also Figs EV5 and EV6.

A Co-localization of MCH and the receptor for CCL2 (CCR2) in the LHA of mice expressing CFP under the promoter of MCH. The overlap of MCH and CCR2 immunoreactivity indicates that CCR2 is expressed on MCH neurons in the LHA.

B–D CCL2 effects on MCH neurons of MCH-CFP knock-in mice recorded in current-clamp mode. Representative trace of the effects of CCL2 on MCH neurons (B). The CCR2 antagonist INCB3344 prevents the small hyperpolarization of MCH neurons elicited by CCL2. Effects of CCL2 at various concentrations, alone or in the presence of the INCB3344 (1 µM) or barium (200 µM) on the membrane potential of MCH neurons (n = 5–16) (C). $^{**}P < 0.01$, $^{***}P < 0.001$, t-test after ANOVA; $^{+}P < 0.05$, $^{++}P < 0.01$, paired t-test, against their own control. Data are expressed as means ± SEM. Discharge pattern of two representative MCH neurons in response to a depolarizing current pulse injection (current pulses applied every 10 s) in control condition and in the presence of CCL2 (D). The control trace is recorded just before the application of CCL2 while the CCL2 trace is recorded 1 min after the beginning of CCL2 application. CCL2 delayed the third action potential (left panel) and induced failures in the action potential evoked in the right panel.

E Effect of CCL2 on KCl-induced MCH release. The perifusion of hypothalamic tissues with 60 mM KCl for 30 min induces an up to 3.1-fold increase in MCH release. CCL2 (100 nM) dramatically blunts KCl-induced MCH release, an effect partially by the addition of INCB3344 (10 µM) (3–5 independent experiments, three chambers per condition in each experiment). $^{*,\$}P < 0.05$, $^{**}P < 0.01$, $^{***}P < 0.001$. * KCl vs. KCl+CCL2 conditions. $^{\$}$ KCl+CCL2 vs. KCl+CCL2+INCB3344 conditions. Data are expressed as mean fold increase in MCH release per chamber vs. basal secretion, ± SEM.

F Effect on MCH-R1 antagonist on LPS- and CCL2-induced weight loss. Data are expressed in mean percentage of weight variation compared to initial body weight at different times (from 2 to 48 h) after acute icv injection of saline (black bar), H6408 (dark blue bar), LPS (red bar), or LPS+H6408 (light red bar), CCL2 (orange bar), CCL2+H6408 (yellow bar) in WT mice (n = 3–12). Data are expressed as means ± SEM. $^{*}P < 0.05$, $^{**}P < 0.01$, $^{***}P < 0.001$; color-coded asterisks indicate a significant difference from the experimental condition assigned to the respective color-coded bar.

Data information: In (E and F), data were analyzed by Student's unpaired two-tailed t-test.
Source data are available online for this figure.

periphery is associated with obesity [59,60], while sickness response is associated with high-grade inflammation (explored here), eliciting different inflammatory signaling in the CNS [61]. Therefore, resolving the paradox about the central effects of CCR2 signaling would require evaluating the response of MCH neurons under conditions that promote either positive or negative energy balance.

In summary, our results demonstrate that brain LPS injection drives CCL2 synthesis that could lead to inhibition of MCH neuron activity through selective CCR2 signaling and subsequently decreases body weight/food intake. This represents the first evidence that a chemokine may directly affect a major orexigenic pathway to contribute to modulate a cardinal response of the sickness behavior.

Materials and Methods

Animals

6- to 8-week-old C57Bl/6J male mice (Janvier Labs, France), MCH-CFP transgenic mice (gift from Prof. J.M. Friedman, Rockefeller University, NY, USA), ORX-CFP transgenic mice (gift from Prof. C. Peyron, Lyon Neuroscience Research, France), and CCR2 KO mice (Jackson Laboratories, USA; strain number B6.129S4-Ccr2tm1Ifc/J) were housed in a room maintained at 22 ± 1°C with a 12-h light/12-h dark cycle and were acclimatized for one week before experiments were performed. For indirect calorimetric studies, mice were housed individually in stainless steel cages. Animals had access to water and chow diet *ad libitum* (SAFE; 2,830 kcal/kg protein 21.4%, fat 5.9%, carbohydrate 51.7% #A03). All of the protocols were carried out in accordance with French standard ethical guidelines for laboratory animals and with approval of the Animal Care Committee (Nice-French Riviera, project agreement no 04464.01).

Drug injections and tissue collection for gene and protein analysis

Drugs were dissolved in saline solution (NaCl 0.9%) for injection. LPS (100 ng to 25 μg; Sigma-Aldrich, France), CCL2 (100 ng; Peprotech, France), INCB3344 (10 μM; MedChem Express, Sweden), and H6408 (10 μM; Sigma-Aldrich) were intraperitoneally and/or stereotaxically injected in WT or CCR2 KO mice, in a total volume of 200 μl (ip) or 5 μl at a rate of 0.5 μl/min (icv) as described in Stereotaxic surgery section. The localization of the icv injection sites was systematically controlled. The INCB3344 was centrally injected since it does not cross the blood–brain barrier. Control mice received saline solution. Experimental groups were injected the same day. Mice body weight was regularly monitored until sacrifice at different times of interest after injection. Hypothalami and cerebella were dissected and processed to study mRNA and protein contents by quantitative RT–PCR and CBA, ELISA or EIA, respectively.

RNA isolation

Total mRNA was isolated according the Chomczynski method as described in Chomczynski *et al* [62] using Fast Prep apparatus (Q-Biogene, France). Two micrograms of total mRNAs was denatured at 65°C for 5 min in the presence of 0.5 mM dNTP and oligodT primers (25 ng/μl; Promega, France).

RT–PCR

Except for RT^2 Profiler PCR arrays (see below) where manufacturer's protocol was followed, reverse transcription of mRNAs was performed using SuperScript® III Reverse Transcriptase (100 U; Life Technologies, France) in a total volume of 20 μl. A negative control lacking RT enzyme was also performed in each assay (NRT). RT and NRT mixtures were diluted 5 times to be used in quantitative real-time PCR experiments.

Polymerase chain reaction array for cytokines and chemokines

RT^2 Profiler Mouse Inflammatory Cytokines and Receptors PCR arrays (PAMM-011Z) (n = 6) were used to analyze the expression of a focused panel of genes. Data analysis was performed using the $\Delta\Delta C_T$ method according to the manufacturer's protocol (SABiosciences/Qiagen, France).

Quantitative real-time PCR

Real-time PCR was performed from reverse-transcribed cDNA samples for relative quantitation of mRNA levels for the genes of interest. Quantitative real-time PCR was performed in a LightCycler® 480 apparatus (Roche, France) using LightCycler® 480 SYBR Green I Master (2×) as described by the manufacturer. Primers were designed using Primer Express 1.5 software (Applied Biosystems, USA) and are detailed in Table EV1. Real-time PCR was performed for amplification of mouse IL-1β, IL-6, TNF-α, CCL2, MCH, ORX, POMC, CART, NPY, AgRP, and GAPDH mRNA. In each assay, PCR were performed in duplicate. Relative quantities of target genes were determined by comparison with results for the control housekeeping gene GAPDH.

Chemokine, cytokine, and neuropeptide quantification

Cerebellar and hypothalamic areas were harvested in ice-cold HBSS (Invitrogen, France) containing protease inhibitor cocktail (Roche, France). Extracts were homogenized by polytron and centrifuged. Supernatants were kept frozen until use. The protein content of the extracts was determined using the Bio-Rad protein assay reagent (Bio-Rad Laboratories, USA). A cytometric bead array (BD™ CBA Mouse Inflammation Kit; BD Biosciences) and a mouse IL-1β ELISA Ready-SET-Go (eBiosciences, France) were used to measure protein levels of IL-6/TNF-α/CCL2 and IL-1β, respectively, according the manufacturers protocols. MCH or ORX peptide levels in tissue lysates or in perifusion samples were measured by enzyme immunoassay kits, as described by manufacturer (refs EK-070-47 and EK-003-30 respectively; Phoenix Pharmaceuticals, USA).

Immunohistochemistry experiments

MCH-CFP and ORX-CFP transgenic mice were perfused with 4% PFA, and brains were collected. Phenotype of MCH-CFP and

ORX-CFP neurons was determined by immunostaining of CCR2 on 40-μm-thick brain floating sections of MCH-CFP and ORX-CFP mice using the anti-rabbit CCR2 antibodies (1:200, [44]), and secondary antibodies conjugated with Alexa Fluor 594 (1/500; Molecular Probes, USA). Confocal microscopy observations were performed with a Laser Scanning Confocal Microscope (TCS SP5, Leica, Germany). We used high-magnification images (objective: ×63, bar 75 μM) to allow a better visualization of overlap between CCR2 and MCH immunoreactivity and absence of overlap between CCR2 and ORX immunoreactivity. To calculate the % of co-localization, we counted the number of CCR2-positive cells on 10 pictures of six independent brain slices from three different mice.

Whole-cell patch-clamp recordings

Whole-cell patch-clamp recording was carried out as previously described [63]. Briefly, hypothalamic slices obtained from brains of 11- to 28-day-old MCH-CFP-KI mice were continuously superfused with a microperfusion system. For current-clamp experiments, we used a K-gluconate internal solution containing (mM): K-gluconate 135, $CaCl_2$ 0.3, $MgCl_2$ 1, HEPES 10, EGTA 1, Mg_2ATP 4, Na_3GTP 0.4, pH adjusted to 7.3 with KOH. Values of access resistance ranged from 12 to 20 MΩ and were left uncompensated. The liquid junction potential between the internal solution (negative) and the standard PBBS solution was 13.2 mV. Membrane potential values given in the text were not corrected for the junction potentials. Measurements were made 2–3 min after obtaining the whole cell to ensure dialysis. MCH neurons were recognized using fluorescence as CFP in these transgenic mice is expressed under the control of MCH promoter thus only in MCH-producing neurons.

Data were digitized at 5–10 kHz using a Digidata interface coupled to a microcomputer running pClamp 9 (Axon Instruments, USA). Current-clamp data were digitized at 0.5 kHz using the same interface. Potentials were digitally filtered at 1–3 kHz. Average data are expressed as mean ± SEM, n = number of neurons.

Perifusion of hypothalamic tissue

Three hypothalamic explants from 8-week-old male C57Bl/6J mice (coordinates: bregma −0.22 to −3.28 mm according to The Mouse Brain in Stereotaxic Coordinates of Paxinos & Franklin) were placed in each perifusion chamber in a controlled environment (37°C, 5% CO_2/95% O_2, constant flow of 0.1 ml/min of MEM (no glutamine, no phenol red, no HEPES; 51200-046 Invitrogen, France) with added 20 μM bacitracin (Sigma-Aldrich), 1 mg/ml BSA (Sigma-Aldrich), 2 mM L-glutamine, and protease inhibitors complete EDTA-free (Roche, France). After a 2-h perifusion to reach equilibrium, the sampling procedure consisted of a 30-min control basal period, a 30-min period during which drugs were added independently or in combination (60 mM KCl, 100 nM CCL2, 10 μM INCB3344) and a 60-min wash with the medium. After each experiment, 60 mM KCl was applied to control the responsiveness of hypothalamic explants. Samples were collected and immediately frozen every 10 min. MCH and ORX concentrations were measured by EIA kit (Phoenix Pharmaceuticals, USA). At least three experiments were carried out for each substance tested (three chambers per group in each experiment).

Stereotaxic surgery

Mice were maintained, anaesthetized through continuous isoflurane (2.5%), then infusion throughout the surgery duration. As soon as the animals were anesthetized, they received an injection of xylazine (Rompun 10 μg/g of BW, Centravet, France). Mice were implanted unilaterally with a chronic 26 stainless steel gauge guide cannula (Plastics One Inc, Roanoke, Virginia, USA) using a Kopf stereotaxic instrument (David Kopf Instruments, Tujunga, USA) to allow icv injection. Unilateral implantation was made into the right lateral ventricle (stereotaxic coordinates relative to Bregma: X: +1 mm; Y: −0.34 mm; Z: −2.5 mm below the surface of the skull) according to The Mouse Brain in Stereotaxic Coordinates of Paxinos & Franklin. Cannulas were maintained in place by dental cement anchored to one stainless steel jewelry screw fixed to the skull. A dummy 33-gauge cannula was inserted to prevent clogging of the guide cannula. At the end of the surgery, mice received an injection of ketoprofen (ketofen 10%, 10 μg/g of BW, Centravet, France). After the surgery, the animals were housed individually for 7 days, during which they were handled, accustomed to the placement of the 33-gauge internal cannula and their body weight monitored daily.

Brain infusion

After 48-h acclimatization in calorimetric cages, non-restrained and conscious mice were weighted and perfused icv by using a catheter connected to the injector inserted into the guide cannula. This catheter was connected to a Hamilton syringe powered by a minipump KDS310 (KD Scientific, Holliston, MA, USA). Mice were accustomed to the operator by frequent handling before the experiment. The first 2 days of the experiment, all mice were perfused with vehicle solution (NaCl, Lavoisier, France) just before the onset of the dark period (18:00 pm; Vt = 2.5 μl; 1 μl/min) for habituation. At the 3rd day of the experiment, mice were divided into three groups and injected either with vehicle solution, LPS (500 ng; Vt: 5 μl), or LPS+INCB3344 (LPS: 500 ng + INCB3344: 10 μM; Vt: 5 μl) at a rate of 1 μl/min just before the onset of the dark period (18:00 pm). The group injected with LPS + INCB3344 was pre-injected with INCB3344 alone (10 μM; Vt: 5 μl; 1 μl/min) one hour before (17:00 pm). Mice were monitored in calorimetric cages for 45 h after those injections.

Indirect calorimetry measurements

Mice were analyzed for whole energy expenditure (EE), oxygen consumption and carbon dioxide production, respiratory exchange rate (RER, CO_2/O_2), food intake (g) and locomotors activity (beam-break/h) using calorimetric cages with bedding, food, and water (Labmaster, TSE Systems GmbH, Bad Homburg, Germany) as described by Joly-Amado *et al* [64]. Fatty acid oxidation was compiled as described by Bruss *et al* [65].

Mice individually housed had free access to food and water *ad libitum* with lights on from 7 am to 7 pm and an ambient temperature of 22 ± 1°C. All animals were acclimated for 48 h in calorimetric cages before experimental measurements.

Whole body composition (fat and lean mass) was measured using an Echo Medical systems' EchoMRI 100 (Whole Body Composition Analyzers, EchoMRI, Houston, USA).

Statistical analysis

Data obtained following icv injections were analyzed with GraphPad Prism 6 using Student's unpaired two-tailed *t*-test. The threshold for significance was $P < 0.05$. For electrophysiology experiments, ANOVA test was used to analyze the differences between groups, followed by a Student's Newman–Keuls *post hoc* test with a threshold of significance of $P < 0.05$ using a statistical software package (SigmaStat 2.03, Jandel Sci). For indirect calorimetric studies, the results are expressed as mean ± SEM. Variance equality was analyzed by Microsoft Excel's *F*-test, and comparisons between groups were carried out using a Student's *t*-test or by a nonparametric Mann–Whitney *U*-test/Wilcoxon's test. When appropriate, analyses of variances were performed followed by a Tukey's *post hoc* test with the appropriate parameters and their interaction as factor. Data with different superscripts letters (a,b,c) differ significantly ($P < 0.05$).

Expanded View for this article is available online.

Acknowledgements

The authors are grateful to Dr. S. Mélik-Parsadaniantz and Dr. A. Réaux Le Goazigo (Institut de la Vision, UMRS 968, Paris) for the gift of the anti-rabbit CCR2 antibody; K.S. Coquelin for the mice lines maintenance; and F. Massa, S. Berthezène, and L. Lucas for their technical support. This work was supported by the CNRS, the Fondation pour la Recherche Médicale (DEQ20150331738 to J.L.N. and DRM20101220421 to N.B. and C.R.), the CAPES/COFECUB Sv 848-15 (to J.L.N.), the SFNEP Research Award (to C.R.), and by the French Government (National Research Agency, ANR) through the "Investments for the Future" LABEX SIGNALIFE: program reference # ANR-11-LABX-0028-01.

Author contributions

CR, NB, and JLN conceived and supervised the study, designed experiments, and wrote the manuscript. CR and NB designed and performed the majority of the experiments, interpreted results, and generated figures and tables. OLT participated to most experiments, developing notably the perifusion set-up with WR, interpreted results, and generated figures and tables. CC performed indirect calorimetric measurements, spontaneous activity, and feeding analyses with RGPD. SL contributed to data analysis of indirect calorimetric experiments and paper writing. MB performed immunohistochemistry experiments; KS and ND participated to qPCR experiments, physiology experiments, and weight measurements of mice. AG performed and analyzed results from electrophysiology experiments. JC contributed to the fax-array analysis. CH discussed results and reviewed the manuscript.

Conflict of interest

The authors declare that they have no conflict of interest.

References

1. Kent S, Bluthe RM, Kelley KW, Dantzer R (1992) Sickness behavior as a new target for drug development. *Trends Pharmacol Sci* 13: 24 – 28
2. McCusker RH, Kelley KW (2013) Immune-neural connections: how the immune system's response to infectious agents influences behavior. *J Exp Biol* 216: 84 – 98
3. Plata-Salaman CR (2001) Cytokines and feeding. *Int J Obes Relat Metab Disord* 25(Suppl 5): S48 – S52
4. Konsman JP, Dantzer R (2001) How the immune and nervous systems interact during disease-associated anorexia. *Nutrition* 17: 664 – 668
5. Serrats J, Schiltz JC, Garcia-Bueno B, van Rooijen N, Reyes TM, Sawchenko PE (2010) Dual roles for perivascular macrophages in immune-to-brain signaling. *Neuron* 65: 94 – 106
6. Dantzer R (2004) Cytokine-induced sickness behaviour: a neuroimmune response to activation of innate immunity. *Eur J Pharmacol* 500: 399 – 411
7. Konsman JP, Parnet P, Dantzer R (2002) Cytokine-induced sickness behaviour: mechanisms and implications. *Trends Neurosci* 25: 154 – 159
8. Wisse BE, Ogimoto K, Tang J, Harris MK Jr, Raines EW, Schwartz MW (2007) Evidence that lipopolysaccharide-induced anorexia depends upon central, rather than peripheral, inflammatory signals. *Endocrinology* 148: 5230 – 5237
9. Chakravarty S, Herkenham M (2005) Toll-like receptor 4 on nonhematopoietic cells sustains CNS inflammation during endotoxemia, independent of systemic cytokines. *J Neurosci* 25: 1788 – 1796
10. Sohn JW, Elmquist JK, Williams KW (2013) Neuronal circuits that regulate feeding behavior and metabolism. *Trends Neurosci* 36: 504 – 512
11. Swanson LW, Sanchez-Watts G, Watts AG (2005) Comparison of melanin-concentrating hormone and hypocretin/orexin mRNA expression patterns in a new parceling scheme of the lateral hypothalamic zone. *Neurosci Lett* 387: 80 – 84
12. Schneeberger M, Gomis R, Claret M (2014) Hypothalamic and brainstem neuronal circuits controlling homeostatic energy balance. *J Endocrinol* 220: T25 – T46
13. Ericsson A, Liu C, Hart RP, Sawchenko PE (1995) Type 1 interleukin-1 receptor in the rat brain: distribution, regulation, and relationship to sites of IL-1-induced cellular activation. *J Comp Neurol* 361: 681 – 698
14. Hanisch UK, Rowe W, van Rossum D, Meaney MJ, Quirion R (1996) Phasic hyperactivity of the HPA axis resulting from chronic central IL-2 administration. *NeuroReport* 7: 2883 – 2888
15. Callewaere C, Banisadr G, Rostene W, Parsadaniantz SM (2007) Chemokines and chemokine receptors in the brain: implication in neuroendocrine regulation. *J Mol Endocrinol* 38: 355 – 363
16. Bittencourt JC, Presse F, Arias C, Peto C, Vaughan J, Nahon JL, Vale W, Sawchenko PE (1992) The melanin-concentrating hormone system of the rat brain: an immuno- and hybridization histochemical characterization. *J Comp Neurol* 319: 218 – 245
17. Leibowitz SF, Wortley KE (2004) Hypothalamic control of energy balance: different peptides, different functions. *Peptides* 25: 473 – 504
18. Nahon JL (2006) The melanocortins and melanin-concentrating hormone in the central regulation of feeding behavior and energy homeostasis. *C R Biol* 329: 623 – 638; discussion 653-655
19. Sakurai T, Amemiya A, Ishii M, Matsuzaki I, Chemelli RM, Tanaka H, Williams SC, Richarson JA, Kozlowski GP, Wilson S *et al* (1998) Orexins and orexin receptors: a family of hypothalamic neuropeptides and G protein-coupled receptors that regulate feeding behavior. *Cell* 92: 573 – 585
20. Huang Q, Viale A, Picard F, Nahon J, Richard D (1999) Effects of leptin on melanin-concentrating hormone expression in the brain of lean and obese Lep(ob)/Lep(ob) mice. *Neuroendocrinology* 69: 145 – 153
21. de Lecea L, Kilduff TS, Peyron C, Gao X, Foye PE, Danielson PE, Fukuhara C, Battenberg EL, Gautvik VT, Bartlett FS 2nd *et al* (1998) The hypocretins: hypothalamus-specific peptides with neuroexcitatory activity. *Proc Natl Acad Sci USA* 95: 322 – 327

22. Banisadr G, Gosselin RD, Mechighel P, Kitabgi P, Rostene W, Parsadaniantz SM (2005) Highly regionalized neuronal expression of monocyte chemoattractant protein-1 (MCP-1/CCL2) in rat brain: evidence for its colocalization with neurotransmitters and neuropeptides. *J Comp Neurol* 489: 275 – 292
23. Rostene W, Kitabgi P, Parsadaniantz SM (2007) Chemokines: a new class of neuromodulator? *Nat Rev Neurosci* 8: 895 – 903
24. Thompson WL, Karpus WJ, Van Eldik LJ (2008) MCP-1-deficient mice show reduced neuroinflammatory responses and increased peripheral inflammatory responses to peripheral endotoxin insult. *J Neuroinflammation* 5: 35
25. Skelly DT, Hennessy E, Dansereau MA, Cunningham C (2013) A systematic analysis of the peripheral and CNS effects of systemic LPS, IL-1beta, [corrected] TNF-alpha and IL-6 challenges in C57BL/6 mice. *PLoS One* 8: e69123
26. Cazareth J, Guyon A, Heurteaux C, Chabry J, Petit-Paitel A (2014) Molecular and cellular neuroinflammatory status of mouse brain after systemic lipopolysaccharide challenge: importance of CCR2/CCL2 signaling. *J Neuroinflammation* 11: 132
27. Conductier G, Blondeau N, Guyon A, Nahon JL, Rovere C (2010) The role of monocyte chemoattractant protein MCP1/CCL2 in neuroinflammatory diseases. *J Neuroimmunol* 224: 93 – 100
28. Brodmerkel CM, Huber R, Covington M, Diamond S, Hall L, Collins R, Leffet L, Gallagher K, Feldman P, Collier P *et al* (2005) Discovery and pharmacological characterization of a novel rodent-active CCR2 antagonist, INCB3344. *J Immunol* 175: 5370 – 5378
29. Guyon A, Conductier G, Rovere C, Enfissi A, Nahon JL (2009) Melanin-concentrating hormone producing neurons: activities and modulations. *Peptides* 30: 2031 – 2039
30. Stanley S, Pinto S, Segal J, Perez CA, Viale A, DeFalco J, Cai X, Heisler LK, Friedman JM (2010) Identification of neuronal subpopulations that project from hypothalamus to both liver and adipose tissue polysynaptically. *Proc Natl Acad Sci USA* 107: 7024 – 7029
31. Conductier G, Brau F, Viola A, Langlet F, Ramkumar N, Dehouck B, Lemaire T, Chapot R, Lucas L, Rovere C *et al* (2013) Melanin-concentrating hormone regulates beat frequency of ependymal cilia and ventricular volume. *Nat Neurosci* 16: 845 – 847
32. Reyes TM, Sawchenko PE (2002) Involvement of the arcuate nucleus of the hypothalamus in interleukin-1-induced anorexia. *J Neurosci* 22: 5091 – 5099
33. Ogimoto K, Harris MK Jr, Wisse BE (2006) MyD88 is a key mediator of anorexia, but not weight loss, induced by lipopolysaccharide and interleukin-1 beta. *Endocrinology* 147: 4445 – 4453
34. Ruud J, Nilsson A, Engstrom Ruud L, Wang W, Nilsberth C, Iresjo BM, Lundholm K, Engblom D, Blomqvist A (2013) Cancer-induced anorexia in tumor-bearing mice is dependent on cyclooxygenase-1. *Brain Behav Immun* 29: 124 – 135
35. Gaykema RP, Goehler LE (2009) Lipopolysaccharide challenge-induced suppression of Fos in hypothalamic orexin neurons: their potential role in sickness behavior. *Brain Behav Immun* 23: 926 – 930
36. Grossberg AJ, Zhu X, Leinninger GM, Levasseur PR, Braun TP, Myers MG Jr, Marks DL (2011) Inflammation-induced lethargy is mediated by suppression of orexin neuron activity. *J Neurosci* 31: 11376 – 11386
37. Quan N, Whiteside M, Herkenham M (1998) Time course and localization patterns of interleukin-1beta messenger RNA expression in brain and pituitary after peripheral administration of lipopolysaccharide. *Neuroscience* 83: 281 – 293
38. Martinon F, Burns K, Tschopp J (2002) The inflammasome: a molecular platform triggering activation of inflammatory caspases and processing of proIL-beta. *Mol Cell* 10: 417 – 426
39. Halle A, Hornung V, Petzold GC, Stewart CR, Monks BG, Reinheckel T, Fitzgerald KA, Latz E, Moore KJ, Golenbock DT (2008) The NALP3 inflammasome is involved in the innate immune response to amyloid-beta. *Nat Immunol* 9: 857 – 865
40. Inoue M, Shinohara ML (2013) NLRP3 inflammasome and MS/EAE. *Autoimmune Dis* 2013: 859145
41. Brown CM, Mulcahey TA, Filipek NC, Wise PM (2010) Production of proinflammatory cytokines and chemokines during neuroinflammation: novel roles for estrogen receptors alpha and beta. *Endocrinology* 151: 4916 – 4925
42. Carrillo-de Sauvage MA, Gomez A, Ros CM, Ros-Bernal F, Martin ED, Perez-Valles A, Gallego-Sanchez JM, Fernandez-Villalba E, Barcia C Sr, Barcia C Jr *et al* (2012) CCL2-expressing astrocytes mediate the extravasation of T lymphocytes in the brain. Evidence from patients with glioma and experimental models in vivo. *PLoS One* 7: e30762
43. Schellenberg AE, Buist R, Del Bigio MR, Toft-Hansen H, Khorooshi R, Owens T, Peeling J (2012) Blood-brain barrier disruption in CCL2 transgenic mice during pertussis toxin-induced brain inflammation. *Fluids Barriers CNS* 9: 10
44. Banisadr G, Queraud-Lesaux F, Boutterin MC, Pelaprat D, Zalc B, Rostene W, Haour F, Parsadaniantz SM (2002) Distribution, cellular localization and functional role of CCR2 chemokine receptors in adult rat brain. *J Neurochem* 81: 257 – 269
45. Sekiya K, Ghatei MA, Lacoumenta S, Burnet PW, Zamir N, Burrin JM, Polak JM, Bloom SR (1988) The distribution of melanin-concentrating hormone-like immunoreactivity in the central nervous system of rat, guinea-pig, pig and man. *Neuroscience* 25: 925 – 930
46. Morrone SR, Wang T, Constantoulakis LM, Hooy RM, Delannoy MJ, Sohn J (2014) Cooperative assembly of IFI16 filaments on dsDNA provides insights into host defense strategy. *Proc Natl Acad Sci USA* 111: E62 – E71
47. Bezzi P, Gundersen V, Galbete JL, Seifert G, Steinhauser C, Pilati E, Volterra A (2004) Astrocytes contain a vesicular compartment that is competent for regulated exocytosis of glutamate. *Nat Neurosci* 7: 613 – 620
48. Block ML, Hong JS (2005) Microglia and inflammation-mediated neurodegeneration: multiple triggers with a common mechanism. *Prog Neurobiol* 76: 77 – 98
49. Jourdain P, Bergersen LH, Bhaukaurally K, Bezzi P, Santello M, Domercq M, Matute C, Tonello F, Gundersen V, Volterra A (2007) Glutamate exocytosis from astrocytes controls synaptic strength. *Nat Neurosci* 10: 331 – 339
50. Mariotto S, Suzuki Y, Persichini T, Colasanti M, Suzuki H, Cantoni O (2007) Cross-talk between NO and arachidonic acid in inflammation. *Curr Med Chem* 14: 1940 – 1944
51. Plata-Salaman CR, Borkoski JP (1994) Chemokines/intercrines and central regulation of feeding. *Am J Physiol* 266: R1711 – R1715
52. Elmquist JK, Coppari R, Balthasar N, Ichinose M, Lowell BB (2005) Identifying hypothalamic pathways controlling food intake, body weight, and glucose homeostasis. *J Comp Neurol* 493: 63 – 71
53. Morris MJ, Chen H (2009) Established maternal obesity in the rat reprograms hypothalamic appetite regulators and leptin signaling at birth. *Int J Obes (Lond)* 33: 115 – 122
54. Xu Y, O'Brien WG 3rd, Lee CC, Myers MG Jr, Tong Q (2012) Role of GABA release from leptin receptor-expressing neurons in body weight regulation. *Endocrinology* 153: 2223 – 2233
55. Joly-Amado A, Cansell C, Denis RG, Delbes AS, Castel J, Martinez S, Luquet S (2014) The hypothalamic arcuate nucleus and the control of peripheral substrates. *Best Pract Res Clin Endocrinol Metab* 28: 725 – 737

56. Panee J (2012) Monocyte Chemoattractant Protein 1 (MCP-1) in obesity and diabetes. *Cytokine* 60: 1 – 12
57. Weisberg SP, Hunter D, Huber R, Lemieux J, Slaymaker S, Vaddi K, Charo I, Leibel RL, Ferrante AW Jr (2006) CCR2 modulates inflammatory and metabolic effects of high-fat feeding. *J Clin Invest* 116: 115 – 124
58. Poon K, Barson JR, Ho HT, Leibowitz SF (2016) Relationship of the Chemokine, CXCL12, to Effects of Dietary Fat on Feeding-Related Behaviors and Hypothalamic Neuropeptide Systems. *Front Behav Neurosci* 10: 51
59. Gregor MF, Hotamisligil GS (2011) Inflammatory mechanisms in obesity. *Annu Rev Immunol* 29: 415 – 445
60. Velloso LA, Araujo EP, de Souza CT (2008) Diet-induced inflammation of the hypothalamus in obesity. *NeuroImmunoModulation* 15: 189 – 193
61. Thaler JP, Choi SJ, Sajan MP, Ogimoto K, Nguyen HT, Matsen M, Benoit SC, Wisse BE, Farese RV, Schwartz MW (2009) Atypical protein kinase C activity in the hypothalamus is required for lipopolysaccharide-mediated sickness responses. *Endocrinology* 150: 5362 – 5372
62. Chomczynski P, Sacchi N (1987) Single-step method of RNA isolation by acid guanidinium thiocyanate-phenol-chloroform extraction. *Anal Biochem* 162: 156 – 159
63. Guyon A, Banisadr G, Rovere C, Cervantes A, Kitabgi P, Melik-Parsadaniantz S, Nahon JL (2005) Complex effects of stromal cell-derived factor-1 alpha on melanin-concentrating hormone neuron excitability. *Eur J Neurosci* 21: 701 – 710
64. Joly-Amado A, Denis RG, Castel J, Lacombe A, Cansell C, Rouch C, Kassis N, Dairou J, Cani PD, Ventura-Clapier R *et al* (2012) Hypothalamic AgRP-neurons control peripheral substrate utilization and nutrient partitioning. *EMBO J* 31: 4276 – 4288
65. Bruss MD, Khambatta CF, Ruby MA, Aggarwal I, Hellerstein MK (2010) Calorie restriction increases fatty acid synthesis and whole body fat oxidation rates. *Am J Physiol Endocrinol Metab* 298: E108 – E116

